Lamellar to Inverted Hexagonal Mesophase Transition in DNA Complexes with Calamitic, Discotic, and Cubic Shaped Cationic Lipids

Li Cui and Lei Zhu*

Polymer Program, Institute of Materials Science and Department of Chemical, Materials, and Biomolecular Engineering, University of Connecticut, Storrs, Connecticut 06269-3136

Received April 8, 2006. In Final Form: June 1, 2006

In this study, we report on the lipid tail molecular shape/size effect on the mesophase self-assembly behaviors of various cationic lipids complexed with double-stranded DNA. The molecular shape of the cationic lipids was tailored from rodlike (a cyanobiphenyl imidazolium salt) to discotic (a triphenylene imidazolium salt), and finally to cubic [a polyhedral oligomeric silsesquioxane (POSS) imidazolium salt]. An increase in the cross-sectional area of the hydrophobic tails with respect to the hydrophilic imidazolium head induced a negative spontaneous curvature of the cationic lipids. As a result, a morphological change from lamello-columnar (L_α^C) phase for the DNA−cyanobiphenyl imidazolium salt (DNA−rod) and DNA−triphenylene imidazolium salt (DNA−disk) complexes to an inverted hexagonal columnar (H_{II}^C) phase for the DNA−POSS imidazolium salt (DNA−cube) complex was observed. The DNA−rod complex had a typical smectic A (SmA) L_α^C morphology, whereas the DNA−disk complex had a double lamello-columnar liquid crystalline phase. However, when the lipid tail changed to POSS, an H_{II}^C morphology was achieved. These morphological changes were successfully characterized by X-ray diffraction and transmission electron microscopy. We expect that these liquid crystalline and crystalline DNA hybrid materials may become potential functional materials for various applications such as organic microelectronics and gene transfection.

Introduction

Double-stranded DNA condensation with cationic species has represented an important process in not only biological systems[1] but also the polymer science field (e.g., coil−globule transition[2]). Especially, DNA−cationic lipid complexes, which are termed as lipoplexes, have received extensive investigations for nonviral gene transfection applications.[3] Thermodynamically, the complexation is driven by the release of small molecule counterions and the electrostatic interaction between negatively charged DNA and positively charged cationic lipids. The efficiency of gene transfection is dictated by many parameters, including cationic and helper lipid classes, surface charge density (or cationic to helper lipid ratio), mesophase morphology of the lipoplexes, cell lines, and so on. In addition, in vivo gene transfection, different from in vitro transfection, is complicated by other factors such as targeted delivery.[4] Understanding the structure−function relationship of cationic lipid-based gene transfection therefore becomes an important research topic.

The equilibrium morphology of lipoplexes is determined by a free energy balance among surface charge density, spontaneous curvature of the lipids, and elastic properties of the lipid bilayers. Two typical equilibrium morphologies have been reported, namely, lamellar (L_α^C, also termed as lamello-columnar in the liquid crystal field) and inverted hexagonal (H_{II}^C) phases. In the lamellar phase, parallel DNA chains were intercalated between positively charged lipid bilayers composed of a mixture of cationic and neutral helper lipids.[5−7] By controlling the ratios of cationic to helper lipids and cationic lipid to DNA, the distance between neighboring DNA could be adjusted.[5] In the H_{II}^C phase, mixed cationic and helper lipids formed a monolayer around DNA and further packed into a hexagonal lattice.[8] Generally, when the lipid spontaneous curvature (c_0) is low (zero) and the bending modulus (k) is high ($\gg k_BT$ where k_B is Boltzmann constant and T is temperature), a L_α^C phase is preferred. On the contrary, if the c_0 is high (negative and $|c_0| \approx 1/R_{DNA}$ where R_{DNA} is the diameter of DNA around 1.0 nm) and k is low ($\ll k_BT$), an H_{II}^C phase is favored.[8]

Since mesophase morphology of lipoplexes is one of many important factors for efficient gene transfection,[8−10] controlling lamellar versus inverted hexagonal phases in lipoplexes has received much attention. To induce a lamellar to inverted hexagonal phase transition, many experimental approaches have been pursued, according to the above-mentioned principles governed by the spontaneous curvature of lipids and bilayer bending rigidity. The first method employed hexagonal forming lipids such as dioleoyl phosphatidylethanolamine (DOPE), which had a negatively curved lipid monolayer of a radius $R = 1.16 \sim 1.59$ nm.[11] When DOPE was mixed with a cationic lipid, dioleoyl trimethylamonium propane (DOTAP), an H_{II}^C phase formed for the DOPE weight fraction above 0.65.[8] Otherwise, the L_α^C phase was obtained. The second method involved incorporation of a short chain alcohol such as hexanol into the lipid bilayers to reduce the bilayer bending rigidity.[8,12] With increasing the hexanol content, a clear first-order $L_\alpha^C \rightarrow H_{II}^C$ transition was observed. In a third method, an increase in the tail length of cationic lipids was utilized.[13] For a series of DNA lipoplexes using pyridium cationic lipids mixed with DOPE, the H_{II}^C was only preferred for

* Corresponding author. E-mail: lei.zhu@uconn.edu. Tel: 860-486-8708.

(1) Elgin, S. C. R.; Workman, J. L. *Chromatin Structure and Gene Expression*; Oxford University Press: New York, 2000.
(2) Baysal, B. M.; Karasz, F. E. *Macromol. Theory Simul.* **2003**, *12*, 627−646.
(3) Tranchant, I.; Thompson, B.; Nicolazzi, C.; Mignet, N.; Scherman, D. *J. Gene Med.* **2004**, *6*, S24−S35.
(4) Kircheis, R.; Wagner, E. *Gene Ther. Reg.* **2000**, *1*, 95−114.
(5) Rädler, J. O.; Koltover, I.; Salditt, T.; Safinya, C. R. *Science* **1997**, *275*, 810−814.
(6) Artzner F.; Zantl, R.; Rapp, G.; Rädler, J. O. *Phys. Rev. Lett.* **1998**, *81*, 5015−5018.
(7) Koynova, R.; MacDonald, R. C. *Nano Lett.* **2004**, *4*, 1475−1479.
(8) Koltover, I.; Salditt, T.; Rädler, J. O.; Safinya, C. R. *Science* **1998**, *281*, 78−81.
(9) Zuhorn, I. S.; Hoekstra, D. *J. Membr. Biol.* **2002**, *189*, 167−179.
(10) Koiwai, K.; Tokuhisa, K.; Karinaga, R.; Kudo, Y.; Kusuki, S.; Takeda, Y.; Sakurai, K. *Bioconjugate Chem.* **2005**, *16*, 1349−1351.
(11) Turner, D. C.; Gruner, S. M. *Biochemistry* **1992**, *31*, 1340−1355.
(12) Krishnaswamy, R.; Raghunathan, V. A.; Sood, A. K. *Phys. Rev. E*. **2004**, *69*, 031905.

10.1021/la060958t CCC: $33.50
Published on Web 06/13/2006

the hydrophobic tails being C_{18} rather than C_{16} in an HEPES-buffered saline (HBS) solution. Other methods were also used to induce the H_{II}^C morphology. For example, pH-controlled DNA condensation in the presence of dodecyldimethylamine oxide (DDAO) induced the H_{II}^C phase at low pH values for DNA-DDAO complex, but the L_α^C phase was formed for the DNA−DDAO/DOPE complexes.[14] Occasionally, the number and length of lipid tails seemed to affect the mesophase morphology of lipoplexes; some single-tailed cationic surfactants were favorable for the H_{II}^C phase.[15,16] Recently, a thermally reversible $L_\alpha^C \leftrightarrow H_{II}^C$ transition was observed in DNA-dodecyltrimethylammonium bromide (DTAB)/DOPE complexes.[17] Furthermore, an $L_\alpha^C \rightarrow H_{II}^C$ transition was achieved by DNA induced lipid mixing of some binary liposomes.[18] Finally, instead of using cationic lipids, anionic lipids together with divalent cations (e.g., Mg^{2+}, Ca^{2+}, Mn^{2+}, etc.) were used to induce DNA condensation, and an H_{II}^C phase was observed.[19,20]

There have been few detailed studies on the tail molecular shape/size induced spontaneous curvature of the cationic lipids to form the H_{II}^C morphology in DNA complexes.[13] In this communication, we report on the molecular shape effect on the mesophase morphology of DNA complexes with cationic lipids having calamitic (cyanobiphenyl), discotic (triphenylene), and cubic [polyhedral oligomeric silsesquioxane (POSS)] tails. Through systematic tailoring of tail molecular shape from rodlike and discotic to cubic and thus the spontaneous curvature of cationic lipids, smectic A (SmA) lamello-columnar to double lamello-columnar, and finally to the H_{II}^C phase transitions are observed in the solid state, as revealed by X-ray diffraction (XRD) experiments. The unique lamellar to inverted hexagonal morphological change is further confirmed by transmission electron microscopy (TEM). It is expected that these liquid crystalline and crystalline DNA hybrids may be potential functional nanomaterials for organic electronics and gene delivery applications.

Experimental Section

The chemical structures of various cationic imidazolium salts having rod, discotic, and cubic tails and their complexes with double-stranded DNA are depicted in Scheme 1. Detailed syntheses of these cationic lipids are described in the Supporting Information. Fish sperm DNA (Na-form) was purchased from USB Corporation (Cleveland, OH) and was extensively purified by dialysis followed by filtration through a 0.20 μm PTFE filter. To prepare DNA complexes, a typical procedure is followed as described elsewhere.[21] Generally, a small amount of the imidazolium salt (∼20 mg) in THF was added slowly into double-distilled H_2O followed by 5-min sonication in a 100 W ultrasonication bath. A uniform solution with slight turbidity was obtained. A saturated aqueous solution of purified DNA in the Na form was added dropwise into an aqueous imidazolium salt solution. The precipitated DNA−imidazolium salt complexes were filtered and repeatedly washed by H_2O to remove free DNA.

Scheme 1. Double-stranded DNA Complexes with Cationic Imidazolium Salts Having (1) Cyanobiphenyl, (2) Triphenylene, and (3) POSS Tails

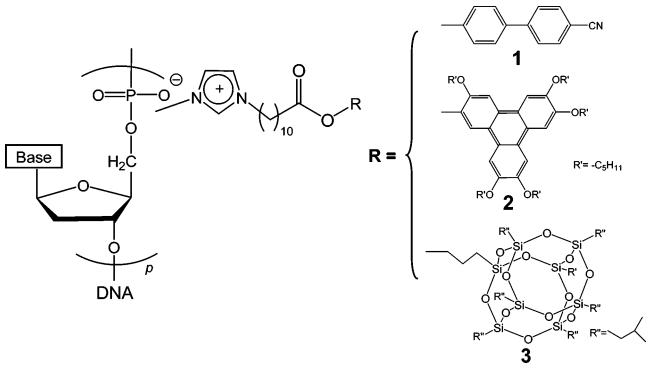

The obtained DNA−imidazolium salt complexes were dried in a vacuum oven at 50 °C for 24 h. To eliminate possible contaminations from extra imidazolium salts, the complexes were dissolved in $CHCl_3$ and precipitated in hexane twice. Finally, the complexes were dried in a vacuum oven at 50 °C for 2 d and stored in a refrigerator.

Two-dimensional (2D) wide-angle X-ray diffraction (WAXD) was performed using an X-ray tube operating at 1.6 kW with the Cr Kα radiation (wavelength $\lambda = 0.229$ nm). WAXD data were recorded at room temperature, using a Bruker AXS area detector with a general area detector diffraction system (GADDS). Dry powder samples sandwiched between two Kapton films were sheared at elevated temperatures and then quickly quenched to room temperature to preserve orientation. In XRD experiments, X-ray beam was directed parallel to the shear direction for the DNA−**1** and DNA−**2** complexes. For the DNA−**3** complex, X-ray beam was along the vorticity direction which was perpendicular to the shear direction. One-dimensional (1D) XRD profiles were obtained by integration of the corresponding 2D WAXD patterns. TEM experiments were performed on a Philips EM300 at an accelerating voltage of 80 kV. Thin sections with a thickness of ca. 70 nm were obtained using a Leica Ultracut UCT microtome equipped with a diamond knife at −30 °C. The thin sections were collected onto 400-mesh copper grids, freeze-dried, and stained by soaking in a 1% uranyl acetate solution for 4 h.[21]

Results and Discussion

In the presence of neutral zwitterionic lipids, double-stranded DNA condenses with cationic lipids to form ordered liquid crystalline mesophases. The L_α^C and H_{II}^C phases are often observed, depending on the spontaneous curvature of the lipids and bending rigidity of lipid bilayers.[8] To tailor the spontaneous curvature of cationic lipids, in this work, we systematically varied the shape of hydrophobic tails from rodlike, to discotic, and finally to cubic. Figure 1 shows the 1D SAXS profiles for DNA complexes with rodlike (**1**), discotic (**2**), and cubic (**3**) cationic lipids, respectively. Differential scanning calorimetry studies during second heating processes showed that the DNA−**1** complex had a glass transition temperature (T_g) at 53 °C and the T_g of the DNA−**2** complex was 36 °C. The POSS crystal melting peak in the DNA−**3** complex was observed at 162 °C, above which a hexagonal columnar phase developed. For all of the samples, the clearing temperatures of the liquid crystalline phases were above their degradation temperatures around 200 °C, as observed by polarized light microscopy. For the DNA−**1** complex in Figure 1A, typical lamellar morphology having a reflection q ratio of 1:2:3 was observed, with an overall layer thickness being 4.53 nm. Considering the diameter of a DNA double helix being ∼2.0 nm and the length of a cyanobiphenyl molecule being ∼1.1 nm, it is reasonable to assume that each layer contains a bilayer of cyanobiphenyl rods and a single layer of DNA (this

(13) Smisterova, J.; Wagenaar, A.; Stuart, M. C. A.; Polushkin, E.; ten Brinke, G.; Hulst, R.; Engberts, J. B. F. N.; Hoekstra, D. *J. Biol. Chem.* **2001**, *276*, 47615−47622.
(14) Mel'nikova, Y. S.; Lindman, B. *Langmuir* **2000**, *16*, 5871−5878.
(15) Tanaka, K.; Okahata, Y. *J. Am. Chem. Soc.* **1996**, *118*, 10679−10683.
(16) Zhou, S.; Liang, D.; Burger, C.; Yeh, F.; Chu, B. *Biomacromolecules* **2004**, *5*, 1256−1261.
(17) Hsu, W.-L.; Chen, H.-L.; Liou, W.; Lin, H.-K.; Liu, W.-L. *Langmuir* **2005**, *21*, 9426−9431.
(18) Caracciolo, G.; Pozzi, D.; Amenitsch, H.; Caminiti, R. *Langmuir* **2005**, *21*, 11582−11587.
(19) Francescangeli, O.; Pisani, M.; Stanic, V.; Bruni, P.; Weiss, T. M. *Eur. Lett.* **2004**, *67*, 669−675.
(20) Liang, H.; Harries, D.; Wong, G. C. L. *Proc. Natl. Acad. Sci. U.S.A.* **2005**, *102*, 11173−11178.
(21) Cui, L.; Miao, J.; Zhu, L. *Macromolecules* **2006**, *39*, 2536−2545.

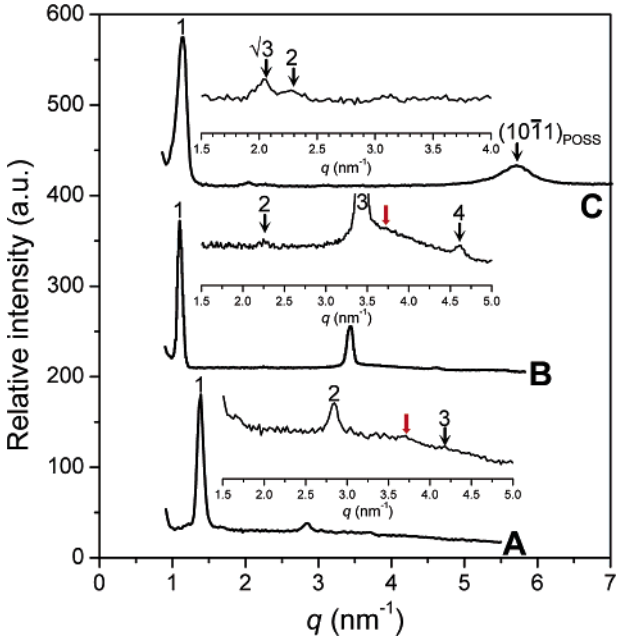

Figure 1. 1D XRD profiles for double-stranded DNA complexes with (A) cyanobiphenyl imidazolium salt, (B) triphenylene imidazolium salt, and (C) POSS imidazolium salt in the solid state. Magnified XRD intensities are shown as insets for panels A−C, respectively.

is consistent with the TEM micrograph in Figure 3A that the white cyanobiphenyl rod layers have a similar thickness as the DNA layers). In the inset of Figure 1A, a broad and weak peak indicated by the red arrow is seen at 3.7 nm^{-1} (*d*-spacing 1.7 nm), which can be attributed to a tight lateral packing of parallel DNA chains sandwiched by bilayers of cyanobiphenyl liquid crystals. For the DNA−**2** complex, lamellar morphology is again observed in Figure 2A, showing a reflection *q* ratio of 1:2:3:4, despite the change of the cationic lipid tail from a rod to a disk. The even-order reflections are weak, which could be a result of the scattering from a three-phase system comprised of DNA, aliphatic spacers/arms, and aromatic triphenylene cores. Near the third-order reflection in the inset of Figure 2B, a broad peak is indicated by the red arrow, and it can be attributed to the lateral packing of DNA and/or triphenylene columns and will be discussed later. The overall layer thickness is 5.98 nm. Since the P5T triphenylene disks have a diameter of 1.7 nm, the lamellar morphology should consist of a single layer of DNA and a bilayer of P5T molecules (this is consistent with the TEM micrograph in Figure 3B that the white P5T layers are thicker than the dark DNA layers). At last, when the tail molecular shape changes to cubic, hexagonal morphology was observed with a reflection *q* ratio being 1:$\sqrt{3}$:$\sqrt{4}$, as seen in the inset of Figure 1C. The (100) reflection of the hexagonal lattice corresponded to a *d*-spacing of 5.56 nm, and thus the inter-DNA distance was 6.42 nm. In Figure 1C, POSS crystal (10$\bar{1}$1) reflection was seen at 5.70 nm^{-1} (*d*-spacing = 1.10 nm).

Although 1D SAXS results suggest a lamellar to cylindrical mesophase transition by varying the tail molecular shape from rodlike and discotic to cubic, detailed liquid crystalline and crystalline structures of these DNA complexes are yet to be determined. Figure 2 shows 2D XRD patterns of shear-oriented DNA lipoplexes at room temperature. In Figure 2A, lamellar reflections are seen on the meridian while the amorphous halo is centered on the equator, indicative of a typical SmA phase for the DNA−**1** complex. For the DNA−**2** complex, up to six orders of layer reflections are seen on the meridian with diffuse vertical striations in the quadrant. Beyond the amorphous halo (around 14.6 nm^{-1}), a pair of relatively sharp reflections with a *d*-spacing of 0.35 nm is observed on the equator, which can be attributed to the face-to-face stacking distance in triphenylene columns. These XRD results suggest a double lamello-columnar (Col_L) liquid crystalline phase for the DNA−**2** complex, with both DNA and triphenylene forming columns.[21] In this unique Col_L phase, however, both double-stranded DNA and triphenylene molecules form liquid crystalline columns, which is in drastic contrast from those reported for DNA complexes with aliphatic cationic lipids.[5−7] The diffuse vertical striations in the quadrant (see the arrow near the center of Figure 2B, corresponding to the broad peak in Figure 1B) suggest that the DNA and triphenylene columns arrange into a pseudooblique packing in each layer with a relatively long lateral correlation length, whereas the correlation length perpendicular to the layers is fairly short. For the DNA−**3** complex, cylindrical mesophase reflections with the *q*-ratio being 1:$\sqrt{3}$ can be seen on the meridian in Figure 2C, suggesting a horizontal alignment of hexagonally packed DNA columns. The POSS (10$\bar{1}$1) reflection arcs are seen on both the equator and the meridian directions with a slightly stronger intensity on the equator. The POSS (11$\bar{2}$0) and mixed (11$\bar{2}$3)/(30$\bar{3}$0) are also observed in the 2D XRD pattern; however, the orientation of these reflections smears. These major reflections for POSS crystals appear at the same positions as those in the pure POSS crystals, indicating the preservation of the trigonal ($R\bar{3}m$) structure[22] in the POSS crystals complexed with DNA. Meanwhile, the asymmetric shape of POSS imidazolium salts complexed with DNA prevented a long-range three-dimensional (3D) packing of the cubic molecules, but they have to crystallize

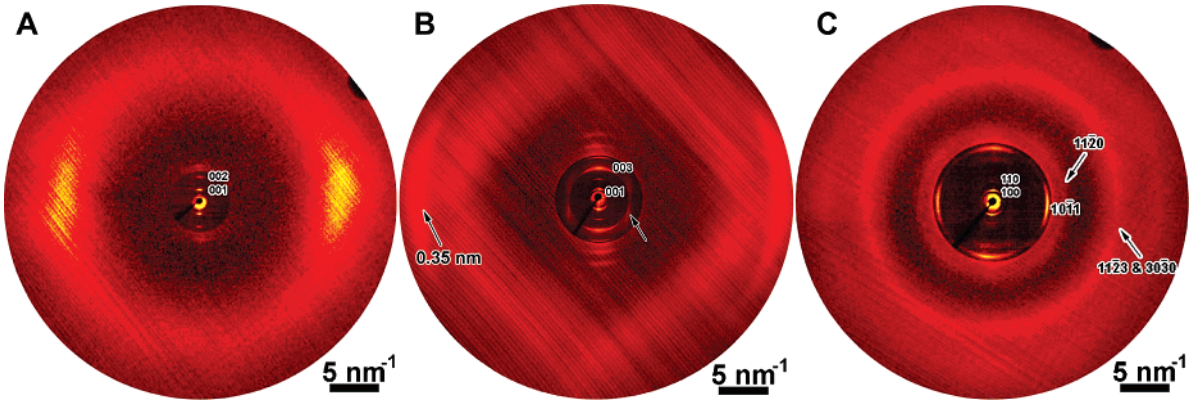

Figure 2. 2D XRD patterns for double-stranded DNA complexes with (A) cyanobiphenyl imidazolium salt, (B) triphenylene imidazolium salt, and (C) POSS imidazolium salt in the solid state. POSS crystal reflections are indexed using the (*hkil*) symbols for a rhombohedral unit cell. Film samples are aligned horizontally for panels A−C.

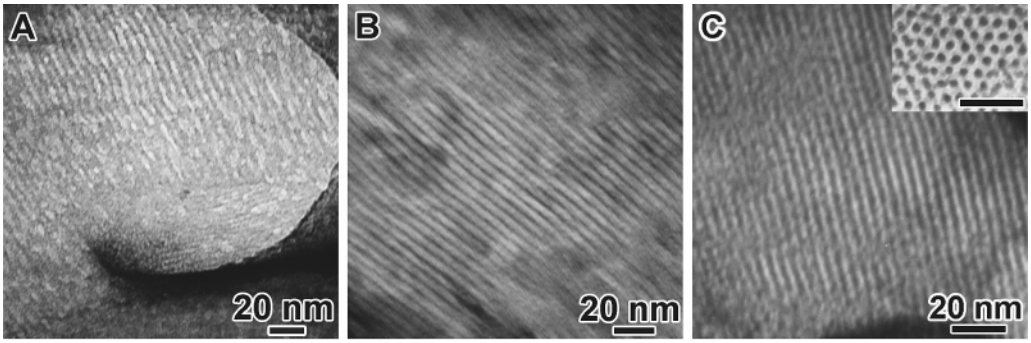

Figure 3. Bright-field TEM micrographs for double-stranded DNA complexes with (A) cyanobiphenyl imidazolium salt, (B) triphenylene imidazolium salt, and (C) POSS imidazolium salt in the solid state. Since uranyl acetate preferentially stains DNA, DNA microdomains appear dark in the micrographs.

into a four-layer lamellar crystal with an ABCA stacking sequence, which is similar to the crystal structure for a disk-cube dyad molecule.[23] Note that the imidazolium heads have to stick out of the crystals from both basal planes in order to form ionic complexes with the DNA phosphate groups. Detailed POSS crystal structure and orientation among hexagonally packed DNA columns are current under investigation and will be published later. Tentatively, a model with four-layer POSS lamellar crystals along three ⟨100⟩ interstitials is assumed.

The unique mesophase transition by varying the molecular shape in the cationic lipid tails was further confirmed by TEM experiments, and results are shown in Figure 3. The DNA microdomains were preferentially stained by uranyl acetate in a 1 wt % aqueous solution. From Figure 3A,B, lamellar morphology was clearly seen for the DNA−**1** and DNA−**2** complexes. For the DNA−**3** complex in Figure 3C, a side-view of parallel DNA cylinders is seen. A head-on view of dark DNA cylinders can be seen in the inset of Figure 3C. The diameter of the dark cylinders is ca. 2 nm, which is consistent with the literature diameter of a double-stranded DNA.

The above results show that the liquid crystalline self-assembly of cyanobiphenyl, triphenylene, and POSS imidazolium salts with DNA does not necessarily have a direct correlation with the "initial" phase behaviors of the end groups. For example, cyanobiphenyl liquid crystals often exhibit a SmA phase, and indeed the DNA−**1** complex has a SmA lamellar morphology. However, triphenylene molecules usually exhibit a hexagonal columnar phase, whereas they self-organize into a double lamello-columnar phase in the DNA−**2** complex. Furthermore, POSS molecules tend to crystallize into 3D trigonal crystals,[22] whereas the DNA−**3** complex forms an inverted hexagonal phase with lamellar POSS crystals between the DNA cylinders.

In summary, by systematically varying the molecular shape in cationic lipid tails, we have successfully achieved morphological transitions in DNA−cationic lipid complexes from a typical SmA lamello-columnar phase for the DNA−rod complex to a double lamello-columnar phase for the DNA−disk complex, and finally to an H_{II}^{C} phase for the DNA−cube complex. Obviously, increasing the tail cross-sectional area with respect to the hydrophilic imidazolium head induced the negative spontaneous curvature, and thus a mesophase transition. Further investigations of POSS crystal growth and orientation are currently underway.

Acknowledgment. This work was supported by NSF CAREER award DMR-0348724, DuPont Young Professor Grant, and 3M Nontenured Faculty Award.

Supporting Information Available: Descriptions of the detailed syntheses of cationic lipids. This material is available free of charge via the Internet at http://pubs.acs.org.

LA060958T

(22) Waddon, A. J.; Coughlin, E. B. *Chem. Mater.* **2003**, *15*, 4555−4561.
(23) Cui, L.; Collet, J. P.; Xu, G.; Zhu, L. *Chem. Mater.* accepted.